PAPER

Check for updates

Lung physiologically based pharmacokinetic modelling to predict sublingual buprenorphine kinetics following oral inhalation

Tobechi Brendan Nnanna, [ID] *[a] Daniel Okwudili Nnamani, [ID] [b]
Elias Bestman Adikwu [ID] [c] and Chisom Anthony Nnanna [ID] [d]

The pulmonary system embodies a heterogeneous yet highly efficient interface for xenobiotic uptake, offering unique translational opportunities for pharmacokinetic modelling. The sublingual route is widely exploited to deliver buprenorphine, a lipophilic partial μ-opioid receptor agonist, while circumventing gastrointestinal degradation and hepatic first-pass metabolism; however, the pharmacokinetics of buprenorphine are marked by pronounced nonlinearity and variability driven by mucosal residence time, dissolution, and involuntary swallowing. In the absence of a native sublingual absorption module within the Open Systems Pharmacology (OSP) ecosystem, this study investigated whether a mechanistically constrained inhalation physiologically based pharmacokinetic (PBPK) framework could serve as a defensible surrogate to recover sublingual buprenorphine kinetics. A human inhalation PBPK model incorporating a 24-generation lung architecture was implemented in MoBi and PK-Sim, integrating morphometric and physiological descriptors with the physicochemical parameters of buprenorphine. Particle deposition was deliberately biased toward the extrathoracic and proximal tracheobronchial regions by selecting reported metered-dose inhaler particle sizes (MMAD ≈ 7.5 μm), thereby emulating sublingual mucosal exposure. The model explicitly resolved particle deposition, epithelial lining fluid dissolution, permeability-limited epithelial transfer, mucociliary clearance–driven swallowing, and systemic distribution, preserving the causal structure. Systemic disposition was described using a two-compartment model, with key parameters estimated through Monte Carlo optimisation. Model performance was evaluated against single-ascending-dose clinical data (2–24 mg) and further verified using independent studies of sublingual tablets and solutions. Across all dose levels (2–24 mg), predicted C_{max} and AUC metrics were recovered within predefined two-fold acceptance limits, with prediction accuracies generally ranging from 73% to 138% for AUC and 81% to 103% for C_{max}. The model robustly reproduced early exposure and peak timing while systematically underpredicting the terminal half-life, consistent with the structural constraints of the systemic disposition model and the absence of explicit mucosal depot or enterohepatic recirculation processes. Sensitivity analysis identified particle dissolution dynamics and mucociliary clearance kinetics as dominant drivers of exposure. In conclusion, this work demonstrates that an open-source inhalation PBPK framework can mechanistically and quantitatively approximate sublingual buprenorphine pharmacokinetics. The approach provides a transparent, extensible surrogate for sublingual absorption, supporting translational modelling and hypothesis generation when route-specific modules are unavailable.

[a]Aston Pharmacy School, College of Health and Life Sciences, Aston University, Birmingham B47ET, UK. E-mail: tnnanna49@gmail.com
[b]Department of Pharmaceutical Sciences, University of Tennessee Health Science Centre, Memphis, TN 38103, USA
[c]Department of Pharmacology and Toxicology, Faculty of Pharmacy, Niger Delta University, Bayelsa State, Nigeria
[d]Department of Pharmacology and Toxicology, Faculty of Pharmacy, Madonna University, Nigeria

1. Introduction

The characterisation of the anatomical and physiological architecture of the human lung presents its uniqueness from the perspective of complex heterogeneity; the lungs feature a gargantuan surface area for absorption, increased vascularisation, and enhanced epithelial membrane permeability in the alveolar region. Accordingly, the risk of first-pass metabolism is lower for xenobiotics administered *via* the lungs, in contrast to orally administered xenobiotics. Moreover, the structural and

functional heterogeneity of the respiratory system encompasses a series of continuously evolving physiological gradients that collectively govern the mechanics of inspiration and expiration. During inspiration, the diaphragmatic contraction and coordinated expansion of the thoracic cage generate negative intrathoracic pressure gradients, driving airflow through progressively branching airways whose geometry, compliance, and regional resistance vary across lung generations.[1] This process is further modulated by spatial heterogeneity in airway calibre, elastic recoil, and regional ventilation, resulting in the non-uniform airflow distribution and time-dependent filling of alveolar units.[2] Conversely, expiration is predominantly passive under resting conditions and is driven by the elastic recoil of lung parenchyma and chest wall structures, with airflow patterns influenced by the airway closure dynamics, smooth muscle tone, and viscoelastic properties of the tissue. Importantly, the transition between inspiratory and expiratory phases introduces cyclic variations in airflow velocity, shear forces, and residence times within the airways, all of which shape particle transport, deposition, and clearance. Together, these bidirectional mechanical processes impose a continuously evolving microenvironment that critically influences pulmonary xenobiotic fate. In this regard, the inhalation route is a critical pathway for administering therapeutic molecules.

Air conduction initiates in the nasal and oral cavities, proceeding through the upper airways (larynx and pharynx) along a branching network of conductive tubes (an inverted tree), ultimately reaching the alveoli, which are defined as miniature air sacs with thin walls enveloped intricately by a capillary network. The branching process consists of 23 levels of branches that culminate in the alveolar sacs, facilitating the placement of 274 to 790 million alveoli.[3] The average number of alveoli is approximately 480 million, with a surface area interfacing with ambient air of around 130 square meters.[4] The surfactant lining of the alveoli facilitates their maintenance of openness. The terminal branches of the alveoli facilitate the diffusion of blood gases, whereas the higher branches do not.

Despite its propensity for use in administering xenobiotics, the lung heterogeneity demonstrates challenges for the formulation and delivery of several bioactive molecules. Pulmonary drug delivery systems have been designed and deployed for this purpose as inhalation devices, which indispensably facilitate inhaled therapeutic molecule deposition at specific lung sites.[5] These consist of dry powder inhalers (DPIs), metered dose inhalers (MDIs), and nebulisers. Particle deposition happening after device-facilitated administration, primarily through oral inhalation, exposes xenobiotics to a clearance propensity at the pulmonary level, occurring through the mucociliary clearance mechanisms, translocation and dissolution from the airway to the other sites, and as well, phagocytosis by macrophages.[6,7] Oral inhalation refers to a drug delivery route whereby a pharmaceutical formulation, aerosolised as particles or droplets or presented in gaseous form, is administered *via* the mouth and entrained into the respiratory tract through controlled inhalation. The fate of the delivered dose is governed by aerodynamic particle characteristics, inhalation manoeuvre, and formulation properties, which collectively determine deposition within the extrathoracic region, the conducting airways, or the alveolar space. This route is widely exploited to achieve local or systemic drug delivery while circumventing gastrointestinal degradation and, where applicable, hepatic first-pass metabolism.[7,8]

From a comparative standpoint, mechanistically, the sublingual mucosa has unique features that facilitate xenobiotic absorption, distinct from the extrathoracic airway epithelium. The sublingual region (floor of the oral cavity) is covered by a thin, richly perfused non-keratinized stratified squamous epithelium.[9] This epithelium is significantly thinner and densely vascularized than the buccal mucosa, thus making the sublingual region an escalated permeability zone in the oral cavity.[9] The absence of a keratinised layer accommodates fewer lipid impediments for xenobiotic transmucosal traversal with capillary proximity, enabling systemic exposure of absorbed biomolecules.[9] Furthermore, the extrathoracic (ET) region of the respiratory tract, encompassing the oral cavity and upper airways, exhibits greater physiological heterogeneity. While portions of the oral cavity share epithelial similarities with the sublingual region, the ET environment is associated with higher fluid turnover, active salivary clearance,[10] and involuntary swallowing,[11] which collectively reduce xenobiotic residence time at the absorptive surface essentially highlighting that transmucosal absorption through these two routes embodies a discursive equivalence.

In addition, the explorative endeavours, albeit of a physiologically based pharmacokinetic (PBPK) modelling conduct, have evaluated the fate of orally inhaled drugs administered through delivery systems. This involves the multiscale mathematical integration of drug physicochemical properties and physiological metrics (tissue volumes, blood flow rates, and organ functions) to mechanistically simulate and forecast the trajectory of xenobiotic behaviour in the body (ADME).[12]

Contemporarily, numerous lung-based PBPK models have been implemented to evaluate the fate of administered xenobiotics from a mechanistic facet and are associated with approach discrepancies to enact a 'fit' for the models' intended purpose. Instances of the model utility accommodate simplifying assumptions to airway characterisation in a bid to attenuate computational costs,[13] intricate compartmentalisation of the lung architecture into distinct regions,[14] dual compartmentalisation of the lung to fluid and tissue regions,[15] as well as a comprehensive account of particle deposition and dissolution processes.[13,16] By model compartmentalisation, description entails a model comprising elements (compartments) that reflect well-mixed tissues or distinct organs for which assumptions regarding state variables are posited (indicating that the variables are uniformly mixed), and no internal structure is presumed. The differential equation that characterises the rate of substance upheavals within a compartment is derived from the mass conservation principle and is founded on either a perfusion-limited or a flow-limited model of disposition.[2]

On the contrary, these PBPK models have been deployed with a distinct use case to mimic the inhalation route as a surrogate pathway to recover the kinetics of sublingually administered therapeutics in several state-of-the-art commercial software (SimCyp) for several drugs. In these implemented models, a therapeutic molecule of culpable utility is sublingually dosed buprenorphine.

Buprenorphine functions pharmacologically as a partial agonist at the mu opioid receptor (MOR) and exhibits significant lipophilicity. It occurs as a semi-synthetic thebaine derivative with a synergistic potency (20–55 times) quadrupling that of morphine.[17] The varied administration routes (intravenous, transdermal, buccal and sublingual) apparently reflect a nonlinear bioavailability typically ranging between 28 and 51%, with substantial inter- and intra-individual variability.[18] This variability arises from several well-documented physiological and behavioural factors including limited and saturable mucosal surface area, dependence on residence time beneath the tongue, salivary dilution, involuntary swallowing, and formulation-dependent dissolution kinetics.[19] Clinical pharmacokinetic studies have repeatedly demonstrated non-linear exposure across the therapeutic dose range, with higher sublingual doses failing to produce proportional increases in systemic exposure.[20–22] One pertinent limitation of sublingual administration is the rapid accumulation of saliva within the sublingual space, which promotes involuntary swallowing and consequently diverts a portion of the administered dose to the gastrointestinal tract, thereby diminishing the benefit of first-pass metabolic avoidance. Given that buprenorphine exhibits poor oral bioavailability (approximately 14%) as a result of extensive hepatic first-pass extraction,[23] sublingual delivery has therefore been strategically adopted to enable effective outpatient dosing in the management of opioid dependence.

Furthermore, its pharmacokinetic properties are extensively documented in the literature.[24–26]

The advent of quantitative extant research reporting inhalation PBPK model implementation as a surrogate pathway to mimic the sublingual absorption of buprenorphine in Simcyp has gained considerable momentum, considering the model-based exploratory, predictive, and translational nuances in several populations of interest.[27–31] These population groups include paediatrics, neonates, adults and pregnant women. However, the predictive parlance, heralding sublingual buprenorphine mimicry using other open-source software inhalation PBPK models, exhibits a queried dearth of substantial argumentation, highlighting limitations that reinforce the importance of elaborate model-based investigations.

The crux of this study aims to examine the predictive ability of an open-source inhalation PBPK model framework using a hypothesis based on the deposition of particles in the oral cavity prior to oral absorption, following a use case scenario of reported metered dose inhaler particle sizes as well as mimicking the sublingual route that shunts absorption of xenobiotics into the blood circulation directly, hence accounting for the bioavailability of drugs within a short time interval.

2. Methodology

2.1 Rationale for implementing a mechanistically constrained inhalation PBPK framework as a surrogate architecture for sublingual drug absorption in the absence of a native sublingual module in MoBi and PK-Sim

The absence of a dedicated sublingual absorption module within the Open Systems Pharmacology (OSP) ecosystem (MoBi and PK-Sim) necessitates a principled and mechanistically defensible alternative for representing sublingual drug input. Rather than introducing an abstract or phenomenological absorption function that lacks physiological interpretability, the present work adopts a deliberate strategy: the repurposing of the mechanistic inhalation PBPK framework in MoBi as a surrogate architecture for sublingual absorption. This decision is backed up with the cognisance that the provided inhalation PBPK model embodies the essential biophysical processes governing sublingual drug uptake, namely, deposition onto a hydrated mucosal interface, dissolution into a thin fluid layer, permeability-limited epithelial transfer, and the generation of a swallowed fraction subject to gastrointestinal handling.

Crucially, this approach preserves the causal structure. The inhalation PBPK model in MoBi is not a "black-box" route descriptor; it explicitly resolves particle deposition mechanisms, epithelial lining fluid (ELF) dissolution kinetics, transepithelial diffusion, mucociliary clearance (MCC), and perfusion-driven systemic distribution. These processes are equally operative albeit in a different anatomical context during sublingual administration. Thus, the inhalation PBPK framework offers a mechanistically homologous scaffold through which sublingual exposure can be reconstructed with scientific integrity, avoiding the epistemic fragility associated with purely computational surrogates.

2.1.1. Conceptualization of sublingual absorption as a split-input system in MoBi. Sublingual administration is fundamentally a split-input system. A fraction of the administered dose undergoes rapid transmucosal absorption directly into the systemic circulation, bypassing hepatic first-pass metabolism, while the remainder is unavoidably swallowed and subsequently exposed to gastrointestinal transit and hepatic extraction. This duality is a defining feature of sublingual pharmacokinetics and underlies the observed variability and nonlinearity in sublingual bioavailability.

The MoBi inhalation PBPK model is inherently structured to represent such split-input behaviour. Following inhalation, deposited particles may either dissolve and permeate locally across the airway epithelium or remain undissolved and be transported proximally via mucociliary clearance to the extrathoracic (ET) region, from which they can be swallowed and handled by the gastrointestinal system. Importantly, this swallowed fraction is not imposed arbitrarily; it emerges as a direct consequence of MCC kinetics (discussed further in section 2.3 [II]) and particle residence times across airway generations. In this respect, MCC serves as a mechanistic analog of the "sublingual tax", the unavoidable loss of dose to the gastrointestinal tract that characterizes sublingual dosing.

By defining the oral cavity/extrathoracic compartment as the effective site of initial deposition and enabling coupling to gastrointestinal absorption, the inhalation PBPK model in MoBi utilised in this study reproduces the structural logic of sublingual delivery without introducing route-specific empirical assumptions. The split between direct systemic input and delayed gastrointestinal contribution is therefore mechanistically generated rather than parameterized, reinforcing the physiological plausibility of the surrogate.

2.1.2.   Particle size as a controllable "route dial": 7.5 μm as a deliberate mucosal delivery choice. Particle size is the primary determinant of regional deposition following oral inhalation and thus functions as a controllable "route dial" within the inhalation PBPK framework. In the present work, the reported aerodynamic particle diameter of approximately 7.5 μm reported in the literature by Bouchikhi *et al.*[32] was intentionally selected not to optimize pulmonary delivery, but to bias deposition toward the extrathoracic and proximal airway regions. Particles within this size regime are dominated by inertial impaction, resulting in preferential deposition within the oral cavity, oropharynx, larynx, and upper tracheobronchial airways.[33] Deep alveolar penetration is minimal, thereby avoiding the near-intravenous systemic kinetics associated with fine respirable aerosols. From a modelling viewpoint, this choice ensures that systemic exposure arises predominantly from mucosal contact and dissolution rather than rapid alveolar uptake, aligning the absorption time course with that observed for sublingual buprenorphine.

Within MoBi, this design choice is operationalized through the deposition algorithms that allocate inhaled mass across airway generations based on the particle size and breathing parameters in a computational conduit. As a result, modifying the particle size produces predictable and mechanistically interpretable shifts in the balance between local absorption and swallowed dose. This tunability is a critical strength of the inhalation PBPK framework, which most likely underpins its suitability as a sublingual surrogate.

2.1.3.   Dissolution at the mucosal interface as the mechanistic bridge between sublingual films and aerosol particles. Regardless of dosage form, whether a sublingual tablet, film, or aerosolized particle; systemic entry requires dissolution into an aqueous environment prior to epithelial permeation. In sublingual dosing, dissolution occurs in saliva and the thin non-keratinized mucosal fluid layer lining the oral epithelium. In the inhalation PBPK model, an analogous process occurs within the epithelial lining fluid. The implemented Inhalation PBPK framework in MoBi explicitly models particle dissolution within the ELF, drawing on dissolution formalisms originally developed for particle-based oral absorption.[34] Dissolved drug then undergoes permeability-limited diffusion across the epithelium into the subepithelium and subsequently into the systemic circulation. This sequence constitutes the mechanistic bridge that most likely unifies sublingual and inhalation-PBPK-based delivery: both are governed by dissolution-rate limited and permeability-controlled flux across a hydrated epithelial barrier.

The equivalence here is not anatomical but functional. By calibrating solubility, particle size, and effective permeability metrics, the inhalation PBPK model can reproduce the temporal characteristics of sublingual absorption while retaining explicit links between parameters and underlying biophysics. This preserves model transparency and supports extrapolation beyond the calibration dose.

2.1.4.   Mucociliary clearance as the formal mechanism generating the swallowed fraction. Mucociliary clearance occupies a central role in establishing the fidelity of the sublingual surrogate. In the inhalation PBPK model, MCC operates as a structured, time-resolved transport process that shifts undissolved particles proximally along the tracheobronchial tree (lung generations) toward the extrathoracic region. Once in the ET compartment, material may be swallowed and subjected to gastrointestinal absorption and first-pass metabolism. This mechanism directly mirrors the fate of undissolved or displaced drug during sublingual administration, where salivary flow and tongue movement lead to progressive swallowing of residual dose. Importantly, MCC kinetics is physiologically constrained by airway geometry and ciliary transport rates, preventing arbitrary tuning of the swallowed fraction. As such, the gastrointestinal contribution emerges organically from the model structure rather than being imposed as a fitted fraction.

By embedding MCC within the inhalation PBPK model surrogate framework, the model captures a defining feature of sublingual pharmacokinetics: the coexistence of a rapid, first-pass avoiding input and a slower, first-pass affected tail. This duality is essential for recovering observed exposure metrics and for maintaining mechanistic credibility.

2.2.   Human lung PBPK model building

Leveraging available published literature IV and oral data from clinical investigations,[20,35] administering buprenorphine whilst adhering to best digitisation practices,[36] a two-compartment model in the PKSolver Excel Addin reported by Zhang *et al.*[37] was utilised to generate parameters for the compartmental transfer micro rate constants (central to peripheral and *vice versa*). Table 1 depicts the input parameters.

A human mechanistic lung PBPK model comprising a 24-generation architecture and human-based physiological parameters was developed. Morphometry information that was based on the Weibel Lung model was adopted.[38] The extrathoracic region (ET) was defined as the cavity of the mouth where the xenobiotic absorption trajectory occurred. The drug particle deposition was predicted by the two-compartment (Fig. 1) typical inhalation path PBPK model published by Pellowe.[39] The particle sizes reported by Bouchikhi *et al.*[32] for 9 metered-dose inhalers (MDIs) were employed to forecast particle deposition in each lung generation. A breath hold time of 2 seconds was simultaneously parameterised as a retention maneuver to improve the residence times of the particle sizes following the conversion to geometric diameters. In addition, the following equation was used to convert aerodynamic diameters (d_{aero}) to geometric diameters (d_{geom}):

Table 1 Buprenorphine data for the oral inhalation PBPK Modelling in MoBi

Parameters	Value	Source
Physicochemical parameters		
Fup	0.04	24
$f_{u,ELF}$	1.00	Eqn (3)
MW(g mol^{-1})	467.64	41
Solubility (mg mL^{-1})	0.0168[a]	42
pk_a	9.62[b]	43
Lipophilicity	4.98	43
$K_{p,u,lung}$	21.43[d]	Optimized
B/P	1	44
Solubility$_{ELF}$	14.87[c]	Optimized
P_{eff} (10^{-4} cm min^{-1})	5.87	PK-Sim
Plasma binding components	AGP	45
Predictive deposition parameters		
Density (g cm^{-3})	1.19	Eqn (2)
GSD (μm)	1.2–1.8	32
MMAD (μm)	7.5	32
Systemic PK parameters in human		
V_d (L)	376.17	
Clearance (L h^{-1})	203	64
$F_{(oral)}$	0.51 (0.28–51%)	25
K_a (hr^{-1})	2.96[c]	Optimized
T_{lag} (h)	0.47[c]	Optimized
K_{el} (hr^{-1})	0.23[c]	Optimized
k_{12}	0.35[c]	Optimized
k_{21}	0.12[c]	Optimized
V_c (L)	1225.00[c]	Optimized
V_{pc} (L)	6225.01[c]	Optimized
Partition coefficient (water/protein)	2107.89[c]	

Abbreviations: V_{pc}, volume of the peripheral compartment; V_d, volume of distribution at steady state; B : P ratio, blood-to-plasma ratio; f_{up}, fraction unbound in plasma; solubility$_{ELF}$, solubility in epithelial lining fluid; GSD, geometric standard deviation; $K_{p,u,lung}$, lung unbound tissue–plasma partition coefficient; MMAD, mass median aerodynamic diameter; V_c, volume of the central compartment.; F_{oral}, oral bioavailability; k_a, first-order absorption rate; T_{lag}, lag time for oral absorption; PK-SIM, PK-Sim standard calculation method; $f_{u,ELF}$, fraction unbound in epithelial lining fluid; k_{12}, first-order constant for transfer from the central compartment to the peripheral compartment; k_{21}, first-order constant for transfer from the peripheral compartment to the central compartment; AGP, α1-acid glycoprotein; K_{el}, elimination rate; V_d, volume of distribution at steady state. [a] Solubility at pH = 7. [b] pK_a of the strongest acid. [c] Parameter optimization was conducted with the Monte Carlo method (standard) in MoBi®. [d] Optimized from eqn (4) in MoBi®.

$$d_{geom} = d_{aero} \times \sqrt{\frac{\rho_{water}}{\rho_{substance}}} \qquad (1)$$

In the study, buprenorphine was investigated as the candidate drug, representing a mimicry of sublingually dosed buprenorphine in the oral cavity.

The buprenorphine density was estimated using the crystallography open database[40] metrics (for buprenorphine free base) with the following equation:

$$\rho = \frac{Z \times M}{N_A \times C_V} \qquad (2)$$

where Z denotes the number of molecules per cell, M is the molecular weight, N_A is the Avogadro number (6.022×10^{-23}); and C_V is the cell volume.

The physicochemical and systemic pharmacokinetic parameters were sourced from the existing literature studies to serve as input for the model. The fraction of unbound xenobiotic in the epithelial lining fluid ($f_{u,ELF}$) was calculated as follows:

$$f_{u,ELF} = \frac{f_{up}}{0.6 + 0.4 \times f_{up}} \qquad (3)$$

where f_{up} denotes the plasma unbound fraction.

The default model was built using cellular permeability estimates derived from the standard PK-Sim methodology[46] which was computed in MoBi.

The lung unbound tissue-to-plasma partition coefficient $K_{p,u,lung}$ was calculated from the published lung tissue-to-plasma partition coefficient ($K_{p,lung}$) data by Takahashi and colleagues,[45] using the following equation:

$$K_{p,u,lung} = \frac{K_{p,lung}}{f_{u,p}} \qquad (4)$$

and subsequently, further optimised using the parameter optimisation tool in the MoBi application.

2.3. Inhalation PBPK model considerations and implementation

General considerations regarding the lung PBPK model account for the heterogeneity of the lung. Following inhalation, xenobiotic particles initially deposit in varying lung locations spatially or eventually reside in the extrathoracic region (oral mucosa or nasal passages). From the initial site of particle landing in the lung, xenobiotic dissolution occurs in the epithelial lining fluid (ELF), consequently being absorbed into the tissue. Mucociliary clearance (MCC) transports the non-dissolved xenobiotic within the tracheobronchial (TB) region of the airways upwardly. Following this, the transport or diffusion of dissolved xenobiotics in the pulmonary region becomes apparent, facilitated by concentration gradients and an eventual distribution to both the lungs and the system (GIT and surrounding tissues) owing to blood circulation.

Theoretical nuances for the lung PBPK framework model implementation account for the following segments:

I. **Mass transfer**: the lung tissues in each generation (1–24) were separated into three sub-compartments, which accounted for the epithelium, subepithelium, and ELF. The following ordinary differential equations were used to describe the passive diffusion of xenobiotics.

For each considered ELF compartment n,

$$V_{ELF,n} \cdot \frac{\partial C_{ELF,n}}{\partial t} = \frac{\partial A_{dissolved}}{\partial t} - P_n \cdot A_{ELF,n}$$
$$\cdot \left(C_{ELF,n} \cdot f_{u,ELF} - \frac{C_{ep,n}}{K_{p,u,lung}} \right) \qquad (5)$$

where $\partial A_{dissolved}/\partial t$ denotes the dissolved amount of the drug per unit time; $V_{ELF,n}$ stands for the volume of ELF compartment n; $A_{ELF,n}$ denotes the surface area of the ELF compartment n; P_n stands for the effective permeability; $f_{u,ELF}$ denotes the fraction unbound in ELF; $K_{p,u,lung}$ denotes the unbound
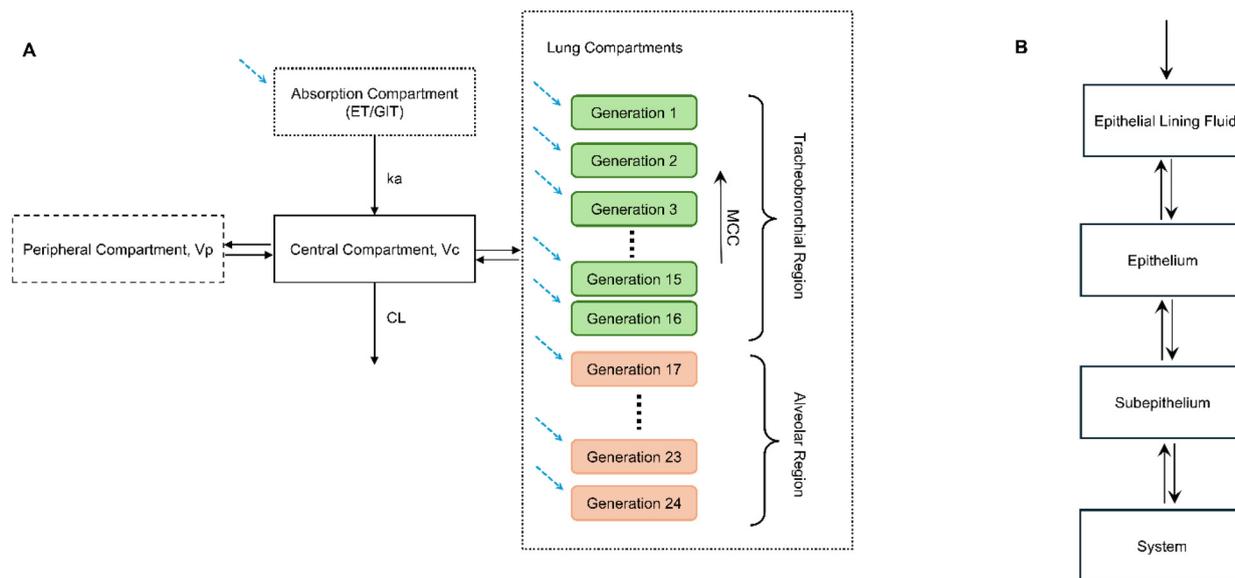
Fig. 1 Two-compartment inhalation PBPK model. (A) General outline (adapted from Wen *et al.*[47]): compartmental absorption is triggered active for oral inhalation and inactive for intranasal inhalation, with lung airways separated into alveolar and TB regions (MCC occurring in the TB region only). Dashed arrows depict inhaled xenobiotic traversal into the system. (B) Lung tissue airway compartments, depicting a further segmentation where the therapeutic molecule migrates to the system through subepithelium. MCC: mucociliary clearance.

tissue-to-plasma partition coefficient for the lung and $C_{\text{ELF},n}$ denotes the concentration of the xenobiotic (buprenorphine) at the ELF compartment n.

For each considered epithelium compartment n,

$$V_{\text{ept},n} \cdot \frac{\partial C_{\text{ept},n}}{\partial t} = P_n \cdot A_{\text{ELF},n} \cdot \left(C_{\text{ELF},n} \cdot f_{\text{u,ELF}} - \frac{C_{\text{ep},n}}{K_{\text{p,u,lung}}} \right) \\ - P_n \cdot A_{\text{ep},n} \cdot \left(\frac{C_{\text{ep},n}}{K_{\text{p,u,lung}}} - \frac{C_{\text{sub},n}}{K_{\text{p,u,lung}}} \right) \quad (6)$$

where $C_{\text{sub},n}$ denotes the concentration of the molecule at the subepithelium compartment n; $V_{\text{ept},n}$ denotes the volume of epithelium compartment n; $C_{\text{ept},n}$ denotes the xenobiotic concentration at the epithelium compartment n; and $A_{\text{ept},n}$ denotes the surface area of the epithelium compartment n.

For each considered subepithelium compartment n, there is,

$$V_{\text{sub},n} \cdot \frac{\mathrm{d}C_{\text{sub},n}}{\mathrm{d}t} = P_n \cdot A_{\text{ep},n} \cdot \left(\frac{C_{\text{ept},n}}{K_{\text{p,u,lung}}} - \frac{C_{\text{sub},n}}{K_{\text{p,u,lung}}} \right) \\ - Q_{\text{BF},n} \left(\frac{X \cdot C_{\text{sub},n}}{K_{\text{p,u,lung}}} \cdot C_{\text{p}}(t) \right) \quad (7)$$

where $Q_{\text{BF},n}$ denotes the blood flow locally; $A_{\text{ep},n}$ denotes the surface area of the epithelial compartment n; $V_{\text{sub},n}$ denotes the volume of the subepithelial compartment n; X denotes the blood-to-plasma ratio; $C_{\text{p}}(t)$ denotes the xenobiotic plasma concentration at time t; and $K_{\text{p,lung}}$ denotes the lung tissue-to-plasma partition coefficient. The depiction of the differential equations applied across the lung regions was adapted from the work of Wen *et al.*[47] The TB region is perfused by bronchial circulation, whereas the alveolar region is supplied by pulmonary blood flow from cardiac output with $Q_{\text{BF},n}$ separately implemented in these dual segments (Appendix section – SI 1).

As illustrated in Fig. 1, the mechanistic lung sub-segments were linked as peripheral compartments to the 2-compartment PK model systemically. Drug particles are administered concurrently at every generation, including the ET compartment, following inhalation.

II. **Lung geometry**: the morphometric data of human airways were adapted from the Weibel lung model.[24] The tracheobronchial (TB) area was represented by generations 1–16 and the alveolar region by generations 17–24 of the lung airways. The ET compartment was regarded as generation 0.

III. **Mucociliary clearance (MCC)**: the movement of pulmonary mucociliary clearance is confined to the TB region. The highest rate of 3.6 mm min^{-1} at the apex of the human lung (generation 1) was used to infer that the MCC rate is proportional to the cross-sectional area of each generation. The duration of particle retention in each airway was assessed due to the variability of mucociliary clearance rates along the airways. Each generation was subsequently partitioned into uniform segments, during which particles remained for an equivalent duration. Particles would traverse the airways till reaching generation 0. The model simulates the mucociliary clearance kinetics by transferring undissolved particles upwards along the ET region every 15 minutes. Utilising each lung slice as a traversal unit, undissolved drug particles are displaced upwards every 15 minutes until they transfer to the ET region and are further absorbed into the gastrointestinal tract compartment.

IV. Drug Dissolution: the particle dissolution methodology integrated into PK-Sim[34] through a computational framework was applied in each unit segment to address the dissolution processes. The assumptions of the inhalation PBPK model influenced the study design based on the following considerations: the epithelial lining fluid solubility is equal to the solubility at the reference pH; the solubility of the xenobiotic across lung generations (24 generations) shows constancy; the dissolution of particles does not consider precipitation; and the lung unbound tissue-to-plasma partition coefficient is equal to the unbound tissue-epithelial lining fluid partition coefficient.

V. Particle Deposition: the mechanistic computation of the model assumes the particle deposition probabilities in cognisance with the extrathoracic deposition mechanisms through inertial impaction, gravitational sedimentation and diffusion. A further assumption of the deposition implementation considers that drug deposition occurs in a single breath cycle in the ELF and ET region.

2.4. Software

The PBPK model development strategy (Fig. 2), computations and simulations were executed utilising the open-source software MoBi and Pk-Sim Version 11.2 (Open Systems Pharmacology-https://www.open-systems-pharmacology.org/). The pharmacokinetic datasets were obtained following a literature search of relevant clinical studies[20] and digitised in line with best practices[36] from snipped figures using WebPlotDigitizer v.3.10 (https://arohatgi.info/WebPlotDigitizer/

). The R software for statistical computing (version 4.3.1) was utilised to computationally parameterise lung and device parameters of the PBPK model. This workflow employed the utility of a constellation of R packages and dependencies (briefly described in the Appendix section), which integrates a myriad of mathematical functions to create relevant outputs for the model. A stepwise implementation (walk-through) of the parameters using the MoBi Interface is highlighted in the SI.

2.5. Model validation

The validation strategy following optimisation involved simulating the reported dose ranges (2 mg, 4 mg, 8 mg, 16 mg, and 24 mg) of buprenorphine in Dong et al.'s[20] single ascending dose (SAD) study. The reported demographics and delineated participant numbers were utilised to replicate the study in a virtual clinical trial domain. In PK-Sim, the clinical study design was based on this study. The model validation is based on the perspectives of model assessment outlined by Rescigno et al.,[48] specifically prediction, retrodiction, and understanding.

2.6. Model application

Following the validation of the model to ascertain its fidelity mechanistically in MoBi and PK-Sim, the data were used to predict the pharmacokinetic parameter profiles across dose ranges (2 mg, 4 mg, 8 mg, 16 mg, and 24 mg) across reported independent clinical studies that administered buprenorphine as a sublingual tablet or a sublingual solution.[19,25,49–53] The evaluated dose ranges were in line with that reported by Dong
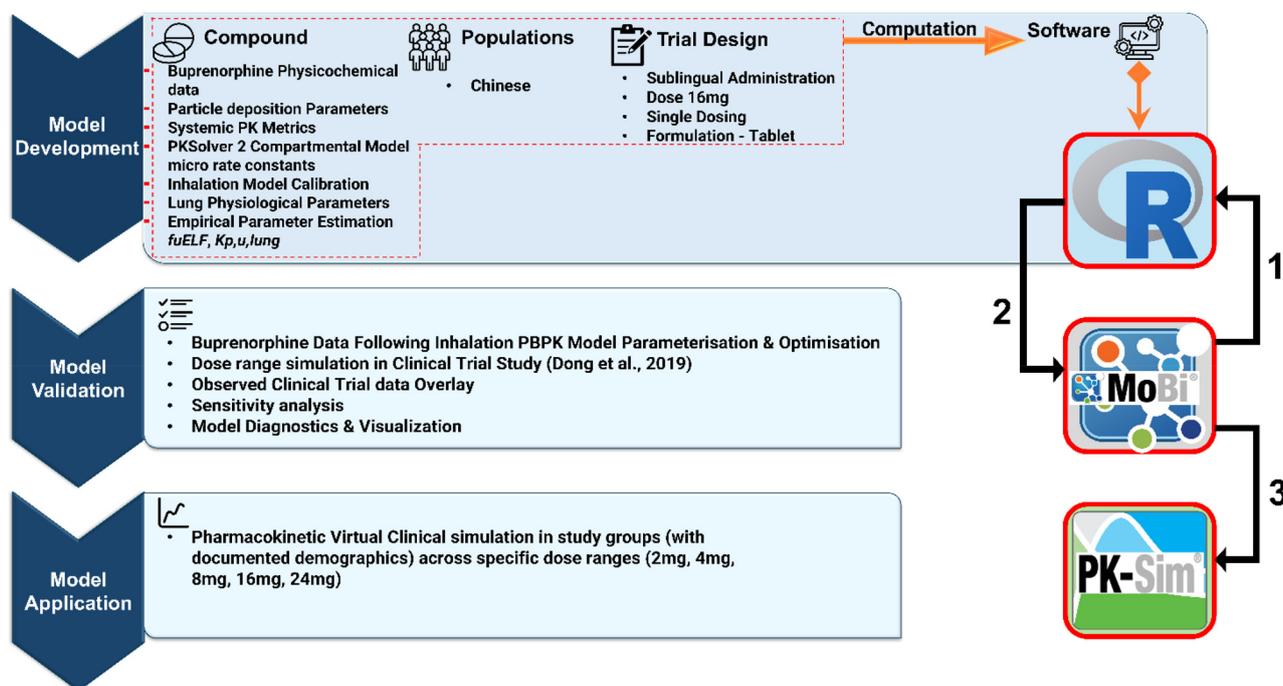

Fig. 2 Inhalation PBPK workflow. In the figure, steps 1–3 represent the inhalation PBPK model walkthrough implementation, which is extensively highlighted in SI 1–section 6.0.

et al.[20] in the SAD open-label phase (that is, 2, 4, 8, 16 and 24 mg, respectively). The inhalation PBPK model pharmacokinetic metric predictions were compared to those reported for each respective clinical investigation. The predicted lung-to-plasma ratio was manually computed by comparing the pharmacokinetic parameters (C_{max}, T_{max}, and AUC) of sublingually dosed (as tablet and solution) buprenorphine reported in the clinical study relative to the inhalation PBPK model-predicted metrics. The virtual trial period was calibrated to the time linked to the last observable concentration reported in the clinical study.

2.7. Parameter identification

Parameter estimations regarding model prediction optimisation to align with the observed data implore an implicit assumption that the specification error of the model is negligible or has a characterisation based on an unbiased error term, thus mitigating the apparent disagreement between predictions and data, essentially producing optimised estimates for realistic numbers. The parameter optimisation conducted was based on select parameters that elucidated a significant impact on the model and in line with the administered dose of sublingual buprenorphine (16 mg) in the clinical study, with a substantiated rationale regarding buprenorphine perfusion into tissues at medium to high doses. The Monte Carlo methodology with a 'standard' optimisation run in MoBi was utilised as the parameter optimisation algorithm.

2.8. Sensitivity analysis

A sensitivity analysis of the sublingual buprenorphine inhalation PBPK model was executed based on a comprehensive set of mechanistically relevant metrics to evaluate the relative influence of critical parameters on pulmonary and systemic exposure, as well as fixed constants on which the mechanistic predictive fidelity of the model runs. The analysis was performed utilising a relative perturbation of parameters of 10%.

2.9. Predictive model performance

An "optimal" predictive performance, defined as the pharmacokinetic parameter prediction in a 2-fold fashion (0.5–2.0) in comparison with the reported studies, was implemented to evaluate the model validation step. In addition, a Visual Predictive Check (after the overlay of observed data) approach[54] was used to assess the model predictive performance. The clarification was achieved by comparing the predicted mean and the 5th and 95th percentiles of the plasma concentration-time profiles with the observed data. Furthermore, goodness-of-fit (GoF) plot assessments were implemented to evaluate the symmetry of distributed predictions (predicted *vs.* observed concentration) along an identity line. The inhalation PBPK model predictive performance was ascertained to be reasonable if the means of the PK metric predicted *versus* observed (P/O ratios) fell between 0.5 and 2 folds (2-fold prediction error range). Moreover, the inhalation PBPK model's prediction following oral inhalation to recover sublingually dosed buprenorphine

metrics was evaluated using predicted *versus* observed AUC, C_{max} and T_{max} and dose *vs.* respective P/O ratio plots.

3. Results

3.1. Inhalation PBPK model building

The open-source typical path mechanistic inhalation PBPK model by Pellowe[39] was utilised in a computational conduit, as the relevant investigative tool for the sublingual route proxy to assess sublingual buprenorphine ADME through oral inhalation based on a hypothesis on reported particle sizes from MDIs reported in the literature.[33] The model incorporated tidal breathing in human subjects, with a breathing frequency of 15 breaths per min as well as an inspiratory-to-expiratory ratio of 1 without pause. Table 1 depicts the drug and model input parameters used in the model building, as well as the referenced literature for buprenorphine-relevant parameters. A reported dose (16 mg) in the clinical trial study[20] was implemented to build the base model, and relevant parameter optimisation iteration based on the Monte Carlo standard algorithm was affected to identify parameters that were optimal for the model performance. The estimated P_{eff} (effective permeability) by the PK-Sim standard method (5.87 × 10^{-4} cm s^{-1}) enabled a better model predictive performance. Physiological parameters of humans were also integrated into the model. The cardiac output was set to 5.2 L min^{-1}, and the maximum MCC rate was calibrated to 3.6 mm per minute at the top of the human lung.

3.2. Model validation and application

Table 2 depicts the pharmacokinetic metric prediction across the dose ranges in the SAD clinical trial study. In Fig. 3(a–e), the predicted *versus* the observed ratios across the investigated dose ranges were within the 2-fold range (0.5–2.0) with a slight deviation visualised for the half-life ($t_{1/2}$) metric (24 mg dose). Moreover, the percentage prediction error (%PE) for the pharmacokinetic parameters (C_{max}, T_{max}, AUC_{inf}, AUC_{0-last}, and $t_{1/2}$) was within the range of −25% to 57.42%.

The prediction accuracy of the PK metric means for C_{max}, AUC_{inf}, and AUC_{0-last} across the dose ranges was within the range of 88%–108%. Likewise, the T_{max} and $t_{1/2}$ prediction accuracies ranged from 43% to 114%, which reflected a slight underprediction by the lung inhalation PBPK model relative to the accuracy threshold established in the study for pharmacokinetic parameters (85%–130%). The dissolution function of the model was activated to account for particle traversal across the oral cavity following oral inhalation. The residence times of the particles in the lung generation and the model-predicted plasma concentration time profiles are documented in the Appendix section (SI 1 and 2).

Tables 3 and 4 depict the resulting output from the simulations of the inhalation PBPK model application against independent clinical investigations that reportedly dosed sublingual buprenorphine (tablet and solution) across stipulated dose ranges. The model predicted metrics were compared with

Table 2 Predicted (orally inhaled) *vs.* observed (sublingual) buprenorphine PK metrics

Dose Parameters	2 mg	4 mg	8 mg	16 mg	24 mg
$AUC_{0\text{-inf}}$ (h ng mL^{-1})					
Predicted	11.5	15.93	34.04	57.56	76.60
Observed	10.9 (4.00)	18.1(4.38)	33.3 (10.8)	55.6 (18.8)	73.0 (18.2)
P/O ratio	1.06	0.88	1.02	1.04	1.04
%PE	−5.50	12.00	−2.22	−3.53	−4.93
$AUC_{0\text{-last}}$ (h ng mL^{-1})					
Predicted	10.46	15.44	33.64	55.21	76.50
Observed	9.78 (3.75)	16.8 (4.12)	31.5 (10.6)	53.1 (18.1)	69.3 (16.7)
P/O ratio	1.06	0.91	1.06	1.03	1.10
%PE	−7.00	8.09	−6.80	−3.97	−10.4
C_{max} (ng mL^{-1})					
Predicted	1.76	2.47	5.12	8.46	11.40
Observed	1.65 (0.418)	2.57 (0.771)	5.00 (1.93)	7.84 (3.26)	11.7 (4.18)
P/O ratio	1.06	0.96	1.02	1.08	0.97
%PE	−6.70	3.90	−2.4	−7.9	2.60
$t_{1/2}$ (h)					
Predicted	16.54	16.54	16.52	37.35	16.52
Observed	22.3 (8.55)	30.1 (10.6)	34.2 (10.8)	34.7 (9.12)	38.8 (12.8)
P/O ratio	0.74	0.55	0.5	1.07	0.43
%PE	25.82	45.04	51.70	−7.64	57.42
T_{max}					
Predicted	0.75	0.75	1	1.25	1.14
Observed	1.00 (0.50–2.00)	1.00 (0.75–1.50)	1.00 (0.50–2.00)	1.00 (0.50–1.50)	1.00 (0.50–1.50)
P/O ratio	0.75	0.75	1	1.25	1.14
%PE	25	25	0	−25	−14

Abbreviations: AUC-area under the plasma concentration–time curve; $AUC_{0\text{-inf}}$-AUC from time zero to infinity; $AUC_{0\text{-last}}$-AUC from time zero to time of the last quantifiable concentration; C_{max}-maximum observed plasma concentration; T_{max}-time to reach C_{max}; $t_{1/2}$-plasma terminal half-life; P/O ratio–ratio between predicted and observed values; and %PE – percentage prediction error calculated as the percentage product of the difference between the observed and predicted parameters relative to the observed parameters. Observed pharmacokinetic parameters are computed as mean (standard deviation).

the observed metrics (AUC, C_{max}, T_{max}) from the respective clinical investigations. Across the independent clinically reported investigations (sublingual tablet and sublingual solution dosing) to which the inhalation PBPK model was applied, the accuracies of the predicted means of the AUC were within 73%–138% (0.5–2.0 fold range) of the observed metrics, as well as that of the C_{max}, which was estimated to be within 81%–103% in the line with the predicted *versus* observed ratio (0.5–2.0). Similarly, the accuracy of T_{max} ranged from 60% to 144%, which apparently reflects a slight underprediction of the model considering the accuracy limits for the study characterisation.

In SI 2, Fig. 1 illustrates the plasma concentration-time profiles of orally inhaled buprenorphine predicted by the mechanistic inhalation PBPK model (solid purple lines), overlaid with observed plasma concentrations following sublingual administration (red circles) across the investigated dose range (2–24 mg). Across all dose levels, the model successfully recapitulated the overall temporal shape of the observed concentration-time profiles, capturing the rapid rise to peak concentration during the early post-dose period and the subsequent multi-exponential decline. At lower doses (2 and 4 mg), the predicted profiles closely followed the central tendency of the observed data throughout both the absorption and post-distribution phases, with minor deviations emerging primarily at later sampling times. At intermediate doses (8 mg), the model

reproduced the magnitude and timing of peak exposure with reasonable predictive fidelity, while modest underprediction became apparent during the terminal phase, reflecting a steeper simulated decline relative to the observed concentrations. At higher doses (16 and 24 mg), the inhalation PBPK model maintained good agreement with observed concentrations during the early and mid-exposure windows, including the attainment of peak levels, but consistently underpredicted plasma concentrations at extended time points, indicating a shorter apparent terminal persistence than that observed clinically. Notably, the degree of divergence in the late phase increased with dose, suggesting that the mechanisms governing prolonged exposure following sublingual administration may not be fully expressed within the current surrogate configuration.

In essence, the profiles demonstrate that the inhalation PBPK framework robustly recovers the dose-dependent exposure dynamics and early systemic kinetics of sublingual buprenorphine, while systematically under-representing the slowest phase of decline, an observation that is concordant with the quantitative underprediction of terminal half-life reported in Table 2.

3.3. Sensitivity analysis

Sensitivity analysis was implemented in MoBi to assess the impact of critical parameters on the AUC_{inf} of the predicted
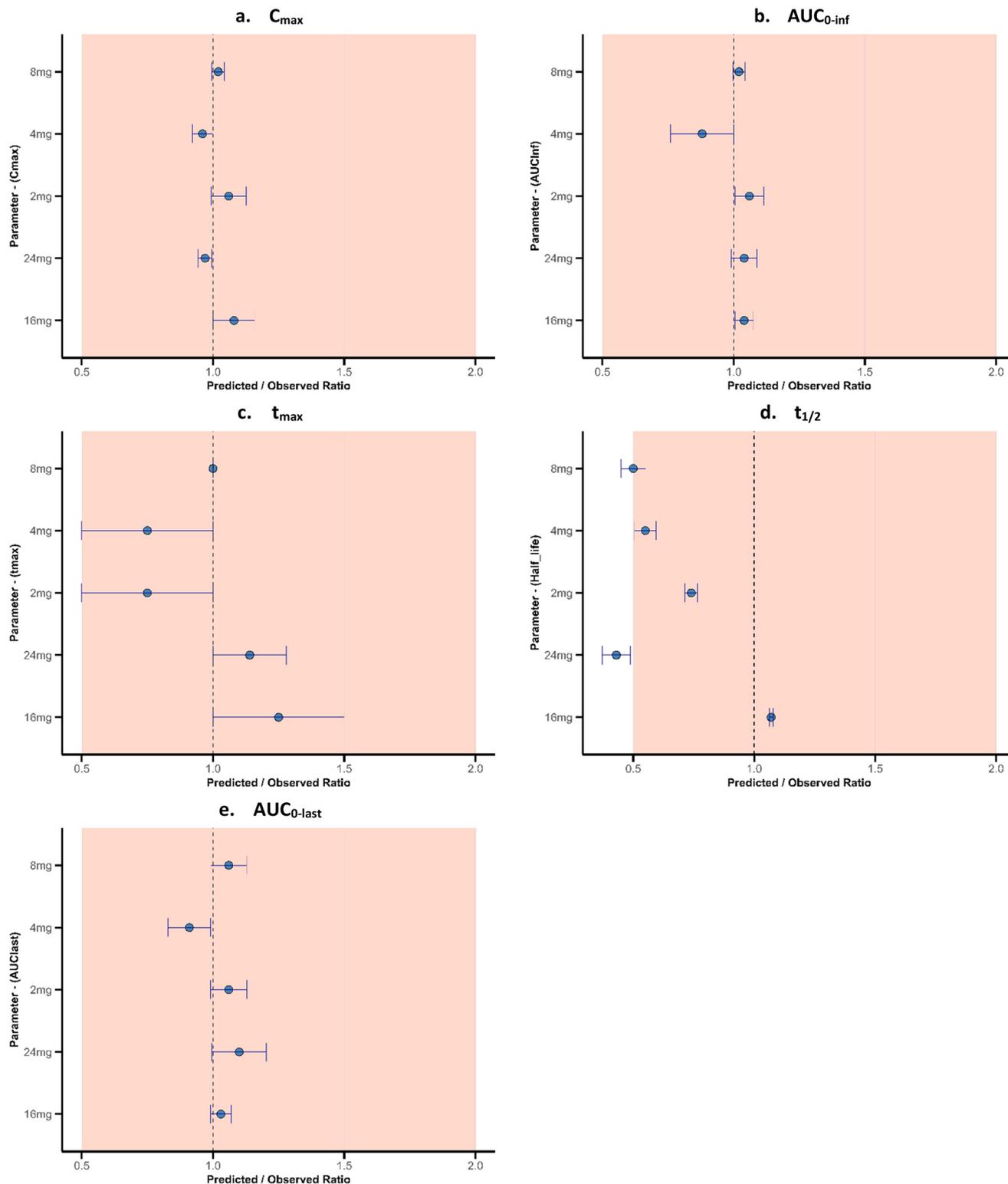
Fig. 3 Forest plots depicting Inhalation PBPK model predicted fold error of Orally Inhaled Buprenorphine PK parameters. Orange shaded areas depicts 2-fold range, dark blue horizontal lines depicting the prediction error.

mean plasma concentration of oral inhaled buprenorphine, as visualised in Fig. 4. The tablet release rate in the ET region (0.790) had a considerable impact on the model performance.

Moreover, the particle radius at the initial time of dissolution was stipulated as 0.597, which further impacted model performance as evaluated by the sensitivity analysis implemen-

Table 3 Inhalation PBPK model Predicted and Observed buprenorphine PK parameters following administration of sublingual tablets

Clinical study	Dose (mg)	Administration path/formulation	N		AUC^a (ng h mL^{-1})	C_{max} (ng mL^{-1})	T_{max} (h)	Female proportion (%)
McAleer et al., 2003[52]	2	Sublingual tablet	27	Predicted	9.21	1.53	1.00	0.0
				Observed	9.05 ± 2.67^b	1.60 ± 0.5^b	1.50 (1.00–3.00)^b	
				P/O ratio	**1.02**	**0.81**	**0.70**	
Ciraulo et al., 2006[49]	4	Sublingual tablet	23	Predicted	11.10	1.90	0.60	30.4
				Observed	9.37 ± 5.35^b	2.00 ± 0.87^b	1.09 ± 0.54^b	
				P/O ratio	**1.17**	**0.95**	**0.60**	
Nath et al., 1999[19]	8	Sublingual tablet	6	Predicted	18.00	3.00	0.94	0.0
				Observed	13.0 ± 5.9^b	2.9 ± 0.5^b	1.2 ± 0.3^b	
				P/O ratio	**1.38**	**1.03**	**0.80**	
McAleer et al., 2003[52]	8	Sublingual tablet	27	Predicted	26.74	4.12	0.91	0.0
				Observed	26.89 ± 7.16^b	4.0 ± 1.2^b	1.02 (0.50–2.00)^b	
				P/O ratio	**1.00**	**1.03**	**0.90**	
Ciraulo et al., 2006[49]	8	Sublingual tablet	23	Predicted	18.05	2.75	0.94	30.4
				Observed	19.92 ± 12.67^b	2.65 ± 1.05^b	1.15 ± 0.49^b	
				P/O ratio	**0.91**	**0.90**	**0.82**	
McAleer et al., 2003[52]	16	Sublingual tablet	27	Predicted	33.82	6.02	1.13	0.0
				Observed	46.19 ± 14^b	6.4 ± 2.6^b	0.75(0.5–2.00)^b	
				P/O ratio	**0.73**	**0.94**	**1.51**	
Chawarski et al., 2005[50]	16	Sublingual tablet	29.5	Predicted	24.71	3.61	1.10	29.5
				Observed	31.10 ± 14.4^b	3.65 ± 2.35^b	1.12^c	
				P/O ratio	**0.77**	**1.00**	**1.40**	
Ciraulo et al., 2006[49]	16	Sublingual tablet	23	Predicted	25.60	4.23	1.0	30.4
				Observed	34.94 ± 20.61^b	4.42 ± 2.05^b	0.94 ± 0.27^b	
				P/O ratio	**0.73**	**1.00**	**1.10**	
Moody et al., 2011[53]	16	Sublingual tablet	11	Predicted	43.00	6.30	1.20	100
				Observed	58.4 ± 24.8^b	6.97 ± 2.98^b	1.00 ± 0.45^b	
				P/O ratio	**0.74**	**0.90**	**1.20**	
Moody et al., 2011[53]	16	Sublingual tablet	20	Predicted	32.00	4.70	1.10	0.0
				Observed	41.9 ± 14.5^b	5.15 ± 1.94^b	1.20 ± 0.50^b	
				P/O ratio	**0.80**	**0.91**	**0.92**	
Chawarski et al., 2005[50]	24	Sublingual tablet	19	Predicted	46.00	6.10	1.14	29.5
				Observed	55.7 ± 24.5^b	6.61 ± 0.67^b	1.13^c	
				P/O ratio	**0.83**	**0.92**	**1.00**	
Ciraulo et al., 2006[49]	24	Sublingual tablet	23	Predicted	46.90	5.0	1.1	30.4
				Observed	48.81 ± 31.0^b	5.41 ± 3.42^b	0.92 ± 0.45^b	
				P/O ratio	**0.96**	**0.92**	**1.19**	

AUC, area under the curve; P/O ratio, ratio between the predicted and the observed value; T_{max}, time to C_{max} attainment. ^{a} AUC$_{0-\tau}$ and AUC$_{0-\infty}$ for single and multiple dose studies. ^{b} Value as reported in the original study. ^{c} Value obtained from van Hoogdalem et al.'s study[55] following Bayesian estimation fitting of the population PK model published by Moore et al.[64] to extracted concentration-time profiles.

Table 4 Inhalation PBPK model Predicted and Observed buprenorphine PK parameters following administration of sublingual solution

Clinical Study	Dose (mg)	Administration Path	N		AUC^a (ngxh mL^{-1})	C_{max} (ng mL^{-1})	T_{max} (h)	Female Proportion (%)
Mendelson et al., 1997[21]	2	Sublingual solution (3 min hold)	6	Predicted	5.94	1.60	0.96	16.7
				Observed	8.75 ± 4.75^b	1.60 ± 0.66^b	1.25 ± 0.42^b	
				P/O ratio	**0.70**	**1.00**	**0.80**	
Mendelson et al., 1997[21]	2	Sublingual solution (3 min hold)	6	Predicted	6.80	1.72	1.0	16.7
				Observed	8.89 ± 5.22^b	1.72 ± 0.87^b	1.62 ± 0.55^b	
				P/O ratio	**0.80**	**1.00**	**0.62**	
Kuhlman et al., 1996[25]	4	Sublingual solution	6	Predicted	15.40	2.0	0.61	0.00
				Observed	17.08 ± 5.76^b	1.98 ± 0.55^b	0.81 ± 0.17^b	
				P/O ratio	**0.90**	**1.00**	**0.75**	
Nath et al., 1999[19]	8	Sublingual solution	6	Predicted	40.04	7.00	1.00	0.00
				Observed	30.5 ± 11.2^b	7.1 ± 2.8^b	0.9 ± 0.3^b	
				P/O ratio	**1.31**	**0.98**	**1.11**	
Chawarski et al., 2005[50]	8	Sublingual solution	18	Predicted	22.00	3.12	1.00	29.5
				Observed	25.4 ± 9.2^b	3.37 ± 1.29^b	1.18^c	
				P/O ratio	**0.87**	**0.93**	**0.85**	
Chawarski et al., 2005[50]	16	Sublingual solution	20	Predicted	32.34	5.03	1.06	29.5
				Observed	35.7 ± 11.3^b	5.25 ± 0.42^b	1.10^c	
				P/O ratio	**0.91**	**0.96**	**0.96**	

Abbreviations: AUC, area under the curve; P/O ratio, ratio between predicted and observed values; and T_{max}, time to C_{max} attainment. ^{a} AUC$_{0-\tau}$ and AUC$_{0-\infty}$ for single and multiple dose studies. ^{b} Value as reported in the original study. ^{c} Value obtained from van Hoogdalem et al.'s study[55] following Bayesian estimation fitting of the population PK model published by Moore et al.[64] to extract the concentration time profiles.
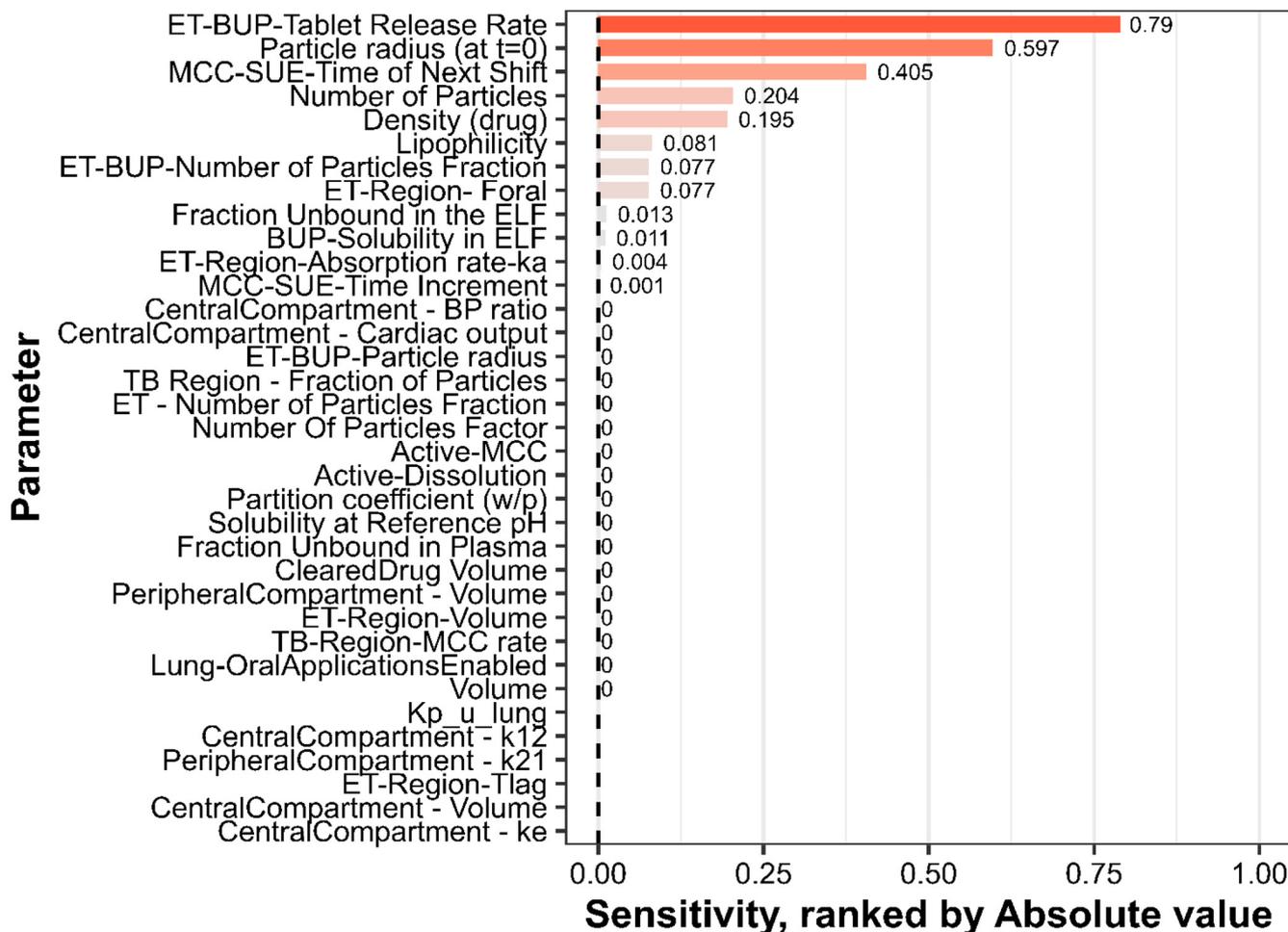
Fig. 4 Sensitivity values indicating the impact of inhalation PBPK parameters on the AUC_{inf} predicted parameters. Abbreviations: BUP−buprenorphine, MCC−mucociliary clearance, F_{oral}−oral bioavailability, BP−blood partition ratio, TB−tracheobronchial, ET-extrathoracic, $K_{p,u,lung}$−lung unbound tissue-to-plasma partition coefficient, T_{lag}−time lag of absorption, k_{12}-transfer constant from the central compartment to the peripheral compartment, k_{21}-transfer constant from the peripheral compartment to the central compartment, ke−elimination rate constant from the central compartment, and w/p−water/protein.

tation. The MCC shift-up-event (SUE) time in the lung gene-ration had a near-half absolute value denoted as 0.405. Other assessed parameters on a physiological, physicochemical, and estimation scale (the unbound fraction in the ELF, lung unbound tissue-to-plasma partition coefficient, $K_{p,u,lung}$) had a minimal impact on the model integrity and performance. An absolute sensitivity value of +1.0 suggests that a 10% incre-ment of the evaluated parameter results in a 10% increase of the corresponding AUC (Fig. 4).

3.4. Predictive model performance

The goodness-of-fit plots depicted in Fig. 5, spanning the investigated dose ranges, highlight the mechanistic predictive performance of the model. Additionally, the plasma exposures of inhaled buprenorphine in the diagnostic plots of the para-meter estimation visualise the confidence interval plots (Fig. 6), which reflect a 95% confidence interval ascertained by the uncertainty linked to the estimated metrics. Similarly, the

comparison plots spanning the illustrations in SI 2-Fig. 2 pre-sents the dose-dependent comparison between orally inhaled buprenorphine model-predicted and observed pharmacoki-netic metrics for sublingually dosed buprenorphine, expressed as predicted-to-observed (P/O) ratios for AUC, C_{max}, and T_{max} across the investigated dose range. For AUC, the majority of data points fall within the predefined two-fold acceptance limits, with a modest non-monotonic trend evident across doses, indicating generally adequate recovery of systemic exposure with minor dose-dependent deviations. The C_{max} P/O ratios remain tightly clustered around unity over the full dose range, demonstrating robust model performance in capturing peak systemic exposure without systematic bias. In contrast, the T_{max} P/O ratios exhibit greater dispersion and a discernible dose-related trend, with underprediction at lower doses and a tendency toward overprediction at higher doses. This pattern suggests that while the model reliably captures exposure mag-nitude, the temporal aspects of absorption display residual
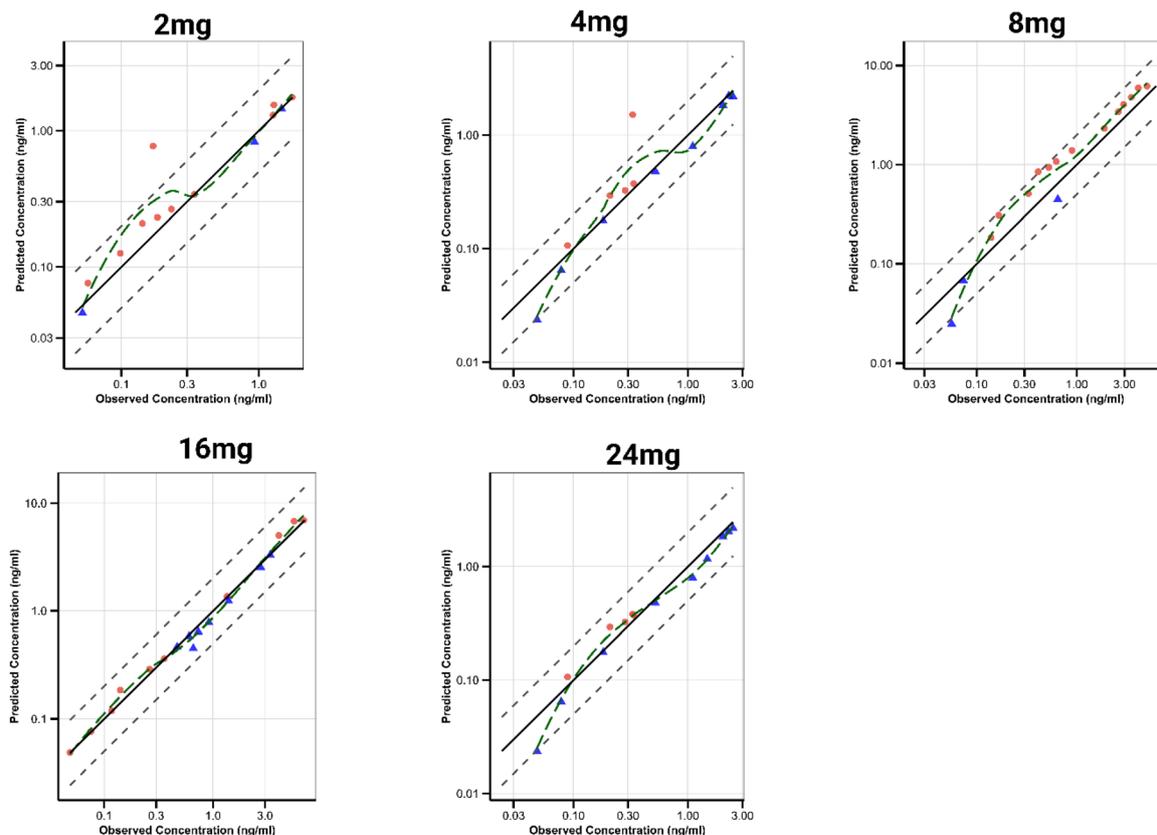
Fig. 5 Goodness-of-fit plots of inhalation PBPK model-predicted concentrations against observed concentrations for dose ranges of 2–24 mg. The solid black line denotes the identity line, and the grey dashed lines denote the two-fold range from the identity line. Vermilion coloured circles depict the concentrations above the identity line. Blue-coloured triangles depict concentrations below the identity line. The green long-dashed line depicts the locally estimated scatter plot smoothing line (LOESS).
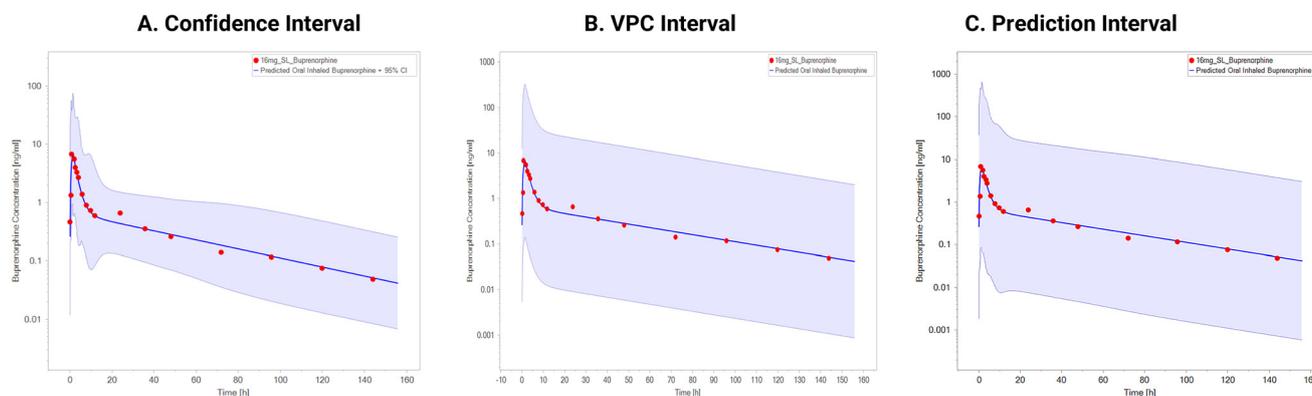

Fig. 6 Diagnostic plots for parameter estimation. SL—sublingual, VPC-visual predictive checking. Interval plot depicts the discrepancy arising from the residual distribution between model predictions and observed data. Prediction interval plot depicts the 95% prediction interval of the model, which integrates the residual distribution variability. Confidence interval plots visualised the uncertainty associated with the optimised metrics.

dose sensitivity. From an intuitive assessment viewpoint, the P/O ratio analyses support the suitability of the inhalation PBPK framework for predicting dose-dependent exposure metrics, while highlighting absorption timing possibly as the principal source of remaining model uncertainty.

4. Discussion

The oral inhalation route serves as a proxy for the absorptive traversal of sublingually dosed xenobiotics, with a paucity of arguments warranting investigation into the mechanistic fide-

lity of the open-source inhalation PBPK model to recover the pharmacokinetic metrics of therapeutics dosed sublingually. This study is the first to leverage oral inhalation xenobiotic administration, using hypothesized particle sizes from MDI aerosols in line with the assumed inhaler device metric characterisation, as a proxy route to mimic the sublingual absorption of buprenorphine across a wide dose range (2–24 mg) using lung PBPK modelling by biasing particle deposition to the TB region in a mechanistic computational conduit.

The crux of the PBPK modelling study was initiated by estimating the two-compartment model PK parameters, as well as the intercompartmental transfer constants documented in Table 1, using the PKSolver Excel Addin.[37] The physicochemical parameters of the xenobiotic under investigation, buprenorphine, were obtained from the relevant studies reported in the literature, as well as the trial demographics of the study participants.[20]

This was followed by a parallel simultaneous computational approach that parameterised the lung PBPK model with the relevant parameters (Table 1 and Fig. 2) initially in MoBi and subsequently parameterised with the lung and deposition metrics in R. PK-Sim was utilised to generate the population study participant demographics in a virtual clinical trial premise and was utilised to simulate the orally inhaled buprenorphine exposure after the parameter optimization sequence (Monte Carlo algorithm – standard run). Furthermore, relevant lung parameters for buprenorphine were estimated utilising eqn (1)–(4). Aerosol particle deposition parameters reported by Bouchikhi et al.[32] were utilised for the inhaled PBPK model parameterisation in R to bias deposition to the tracheobronchial lung segments.

The 51% bioavailability was implemented for the model development using the 16 mg dose in Dong et al.'s study.[20] However, in the validation stage the bioavailability metric was varied (33.9% CV) to accommodate the ranges (28%–51%) reported in the literature for the model application stages across several dose ranges (2–24 mg) within the study cohort.

In the model application/verification stage, the optimised inhalation PBPK model parameters were used to simulate against 18 reported digitised clinical study concentration-time profile data (320 healthy individuals) for sublingually dosed buprenorphine with similar dose ranges (2–24 mg) used for the validation stage as well as with varied formulations (sublingual tablet and solutions). The mean P/O ratios of AUC, C_{max} and T_{max} (Tables 3 and 4) were assessed to be within the 2-fold prediction error range. The comparison plots (SI 2- Fig. 2) indicated an unbiased prediction of the stipulated PK parameters, except for the T_{max} metric elucidating a dose-related trend, with underprediction at lower doses and overprediction toward higher doses. A ± 50% discrepancy in the model-predicted PK parameter was deemed plausible given the variability of sublingual buprenorphine.

The sublingual route as well as the inhalation route of drug administration offer numerous advantages, notable of which is an increased efficacy, and escalated systemic presence of drugs following administration is tantamount.[56] Several com-

parisons have been documented in the literature on the speculated particle deposition sizes for several inhalers.[56]

The inhalation PBPK model utilised in this study was developed upon numerous partial differential equations to account for particle deposition mechanisms, which include gravitational sedimentation, inertial impaction, and diffusion. These mechanisms, as described in the literature, account for the deposition of particle sizes in various lung segments whilst assuming the same lag time for both the tablet and solution. The contribution of each mechanism to the deposition is dependent on the airway obstruction degree, lung architecture, distribution of particle sizes and subject breathing pattern.[33]

The converted aerosol mass median aerodynamic diameter (MMAD) of the MDIs (7.5 μm) to the geometric diameters (6.9 × 10^{-6}) suggests that the gravitational sedimentation (for particles in the size range of 1–8 μm) and inertial impaction (for particles of >5 μm) were the likely mechanisms for particle deposition in the lungs. Sedimentation is a temporal process that transpires when gravitational force exerts influence on a particle, resulting in its gradual displacement from the airstream trajectory. If the particle's weight exceeds the effect of buoyancy exerted by the liquid, it will deviate from its initial streamline trajectory.[57] As the particle descends, it encounters drag from the fluid, resulting in a rapid attainment of terminal settling velocity. On the contrary, deposition critically depends on the parameters of inhalation, notably breath-hold pause, inhalation flow rate and the inhaled volume. Moreover, as highlighted by Arora and colleagues,[58] xenobiotic delivery through pressurised MDIs ought to incorporate a slow flow rate.

The simulation of the PK profiles across the dose ranges in the clinical study (Table 2 and Fig. 1 – SI 2) assessed the predictive ability of the inhalation model to recover the pharmacokinetic parameters of sublingual buprenorphine kinetics. In line with the arbitrary standards used to assess the model performance (85%–130%), the $t_{1/2}$ metric was under-predicted (Fig. 3). The half-life of buprenorphine varies depending on the route of administration: 37 hours (F = 28%–51%) for the sublingual tablet, 26 hours (F = 15%) for a transdermal patch, 2 hours (F = 100%) for intravenous use, and 28 hours (F = 46%–65%) for a buccal film.[18] Under-prediction of this metric could be accounted for by the epistemic uncertainty attributes of the model, that is, an incomplete knowledge of the model under investigation. The percentage prediction error of the PK metrics (Table 2) that ranged from −14% to 57.42% could be accounted for from the viewpoint of aleatoric model uncertainty.[59] In this context, this signifies a fundamental characteristic of the system, thus affecting the disparity in the assessed metrics. The discrepancies illustrated in Table 2 and Fig. 3 can be further corroborated by the assertions made by Clewell III et al., whose work argues that "the scale of comprehensiveness integrated into a model is necessarily a compromise between biological preciseness and parsimony".[60] Furthermore, the systematic underprediction of the terminal half-life ($t_{1/2}$) observed in the present analysis (Table 2) can be mechanistically accounted for as a structural consequence of the eigenvalue

constraints imposed by the optimised systemic micro-rate constants within the two-compartment disposition framework. In a linear mammillary system, the terminal phase is governed by the terminal disposition rate constant (β), which is fully determined by the interplay between elimination (k_{10}) and inter-compartmental exchange rate constants (k_{12}, k_{21}).[61] Given the optimised values obtained herein, the resulting terminal disposition rate constant yields a terminal half-life of approximately 16–17 hours, which aligns closely with the model-predicted values across doses but remains shorter than the apparent terminal half-life reported following sublingual buprenorphine administration. This discrepancy indicates that the observed clinical terminal phase is not solely reflective of systemic elimination and distribution kinetics but likely incorporates slower processes that are not explicitly represented within the current inhalation PBPK model surrogate architecture. In particular, transmucosal (buccal and sublingual) buprenorphine administration has been previously associated with prolonged terminal decline relative to intravenous dosing, a phenomenon plausibly attributed to shallow depot behaviour within the oral mucosa and surrounding tissues, whereby drug sequestration in oral tissues[25,62] decreases the concentration gradient that propels sublingual buprenorphine absorption and gradual re-entry into the systemic circulation effectively extends the apparent terminal phase. In addition, extensive tissue distribution and slow redistribution from deep peripheral compartments have been reported for buprenorphine, suggesting that a two-compartment systemic model may insufficiently capture the slowest kinetic modes governing late-time concentrations. Within the present inhalation PBPK-based surrogate, rapid dissolution in the epithelial lining fluid and comparatively fast transmucosal transfer may further bias the system away from absorption-limited or depot-driven terminal behaviour, thereby allowing the terminal disposition rate constant of the systemic model to dominate the terminal slope. Collectively, these considerations support the interpretation that the underpredicted $t_{1/2}$ arises not from parameter misspecification *per se*, but most likely from a structurally constrained representation of the slowest kinetic processes. Accordingly, future research should prioritise the explicit incorporation of a mucosal retention or depot sub-compartment within the extrathoracic region, as well as the evaluation of extended systemic distribution architectures, to determine whether the clinically observed terminal half-life can be recovered without compromising the model's fidelity for exposure metrics such as C_{max} and AUC. Such extensions would most likely preserve mechanistic consistency while enabling the model to express slower processes that are biologically plausible for sublingual buprenorphine disposition kinetics and are currently not elucidated within the present modelling framework. The inherent discrepancies present may provide additional insights into the underprediction of the T_{max} metric, as disparities may arise between the quantity administered and the amount effectively absorbed during the clinical study. Interindividual variability may likewise contribute to the model overprediction of the T_{max} metric during the validation

and application phases, as clinical evidence indicates that following sublingual buprenorphine administration,[63] substantial variability exists in the proportion of dose that is swallowed *versus* absorbed sublingually. In practice, some individuals may deviate from dosing instructions by crushing or pulverising the formulation prior to swallowing, while others may retain the dosage form sublingually for variable durations, or administer the tablet intact *versus* divided or crushed. Such behavioural and administration-related heterogeneity directly influences the effective absorption pathway and consequently the time required for buprenorphine to reach peak plasma concentrations. This interpretation is further supported by the findings of Kuhlman *et al.*, who reported a wide dispersion in observed T_{max} values for buprenorphine, ranging from approximately 40 minutes to 3.5 hours, underscoring the intrinsic variability of this metric in clinical settings.[25]

Incorporating the morphometry and anatomical attributes of the lung heterogeneity enabled model-predicted pharmacokinetic metrics of the dose ranges across diverse tissues and segments. The estimated $K_{p,u,lung}$ was optimised to further allow the extensive partitioning in the lungs, but the optimal value ought to be assessed with caution due to its propensity for the underestimation of tissue affinity.

Several drawbacks mar the course of this investigation. First, translation from healthy volunteers to diseased populations is not addressed within the present model. Pathophysiological attributes of the target disease state, including disease-specific alterations in lung structure, airway mechanics, mucociliary function, and regional perfusion, would need to be explicitly integrated as mechanistic knowledge advances regarding how such factors modulate pulmonary drug disposition and systemic exposure. Second, the model's lack of explicit representation of enterohepatic recirculation constitutes a notable limitation, particularly given that buprenorphine undergoes partial metabolism *via* UDP-glucuronosyltransferases and that its glucuronide conjugate may be regenerated to the parent compound through bacterial deconjugation within the intestine, allowing subsequent reabsorption and prolonged systemic exposure,[52] and thus, subsequently lending substantive perspective albeit from a theoretical account for the underpredictions (SI 2 – Fig. 1) for the terminal elimination phase at high doses. Third, the optimised model parameters specifically used for this study could be subject to under-the-hood computational aberrations that may influence the implemented Monte-Carlo algorithmic performance when executed with separate computational platforms. Furthermore, the K_p values employed to characterise buprenorphine distribution within lung tissue were derived from rat studies, as corresponding human tissue partition coefficients have not been reported. Notably, tissue distribution in the rat experiments was not quantified under rigorously defined steady-state conditions,[45] thereby constraining the reliability of the K_p estimates implemented in the present model. Nonetheless, despite these translational limitations, the PBPK framework using these K_p values adequately reproduced the observed concentration time profiles, and the

empirically derived steady-state volume of distribution (V_{ss}) of 5.37 L kg^{-1} approximates the clinically reported value of 4.95 L kg^{-1}.[25]

5.   Conclusion

The predilection of the modelling study highlights the frugal possibility and investigative use case of an open-source inhalation PBPK model to mimic the sublingual absorption pathway of administered dose ranges of sublingual buprenorphine albeit with a plausible posit of particle size diameters from investigated MDIs. The inhalation PBPK model recovered the PK metrics across each investigated dose when compared to the data reported in the clinical study, in agreement with the dosing as well as sampling protocols therein. This lends support to multifaceted modelling endeavours in the sublingual absorption route mimicry and, in essence, conceives novelty in the possibility of leveraging the mechanistic open-source inhalation PBPK model as a surrogate absorption pathway for sublingually dosed buprenorphine or other xenobiotics.

Author contributions

T. B. N. was responsible for conceptualisation, supervision, methodology, software computation, formal analysis, investigation, data curation, drafting the original manuscript, visualisation, and project administration. E. A. contributed towards resources, validation, and critical review and editing. D. O. N. undertook data digitization, formal analysis, data curation, and review and editing. C. A. N. contributed to the literature search, project administration, and manuscript review and editing. All authors approved the final version of the manuscript.

Conflicts of interest

There are no conflicts to declare.

Abbreviations

CI	Confidence interval
ELF	Epithelial lining fluid
ET	Extrathoracic
$f_{u,ELF}$	Fraction unbound in epithelial lining fluid
f_{up}	Fraction unbound in plasma
GoF	Goodness-of-fit
GSD	Geometric standard deviation
$K_{p,lung}$	Tissue-to-plasma partition coefficient for the lung
$K_{p,u,lung}$	Unbound tissue-to-plasma partition coefficient for the lung
MCC	Mucociliary clearance
MMAD	Median mass aerodynamic diameter
P_{eff}	Effective permeability
PBPK	Physiologically based pharmacokinetic
PK	Pharmacokinetics
TB	Tracheobronchial
V_{ss}	Volume of distribution at steady state
VPC	Visual predictive checking
T_{max}	Time to maximum concentration
$t_{1/2}$	Half-life
C_{max}	Peak concentration
AUC	Area under the curve
MOR	mu opioid receptor
F	Bioavailability
MDI	Metered dose inhaler
ADME	Absorption, distribution, metabolism and excretion.

Data availability

All computational models, simulation codes, and parameterisation scripts underpinning this physiologically based pharmacokinetic investigation are openly accessible *via* the Open Systems Pharmacology repository (*Inhalation-Model*) on GitHub at Open-Systems-Pharmacology/Inhalation-model: implementation of inhalation model in MoBi. Pharmacokinetic datasets utilised for model building and validation were obtained from previously published studies as cited in the manuscript. Additional datasets (visualised in the manuscript) were generated during the simulation endeavour. These are available from the corresponding author upon request.

Supplementary information (SI) is available. See DOI: https://doi.org/10.1039/d5pm00266d.

Acknowledgements

References

1 J. E. Hall, *Guyton and Hall Textbook of Medical Physiology*, Elsevier Health Sciences, 2010. Guyton Physiology.

2 J. J. Batzel, F. Kappel, D. Schneditz and H. T. Tran, Respiratory Modeling, in *Cardiovascular and Respiratory Systems [Internet]*, 2007, pp. 45–103.

3 M. Ochs, J. R. Nyengaard, A. Jung, L. Knudsen, M. Voigt, T. Wahlers, *et al.*, The Number of Alveoli in the Human Lung, *Am. J. Respir. Crit. Care Med.*, 2004, **169**(1), 120–124.

4 E. R. Weibel and H. Hoppeler, Modeling Design and Functional Integration in the Oxygen and Fuel Pathways to Working Muscle, *Cardiovasc. Dis.*, 2004, **4**(1), 5–18.

5 A. V. Singh, A. Romeo, K. Scott, S. Wagener, L. Leibrock, P. Laux, *et al.*, Emerging Technologies for In Vitro

Inhalation Toxicology (Adv. Healthcare Mater. 18/2021), *Adv. Healthcare Mater.*, 2021, **10**(18), 2170082.

6 W. Liang, H. W. Pan, D. Vllasaliu and J. K. W. Lam, Pulmonary Delivery of Biological Drugs, *Pharmaceutics*, 2020, **12**(11), 1025.

7 J. M. Borghardt, C. Kloft and A. Sharma, Inhaled Therapy in Respiratory Disease: The Complex Interplay of Pulmonary Kinetic Processes, *Can. Respir. J.*, 2018, **2018**(1), 2732017.

8 B. L. Laube, H. M. Janssens, F. H. C. de Jongh, S. G. Devadason, R. Dhand, P. Diot, *et al.*, What the pulmonary specialist should know about the new inhalation therapies, *Eur. Respir. J.*, 2011, **37**(6), 1308–1417.

9 E. Mazzinelli, I. Favuzzi, A. Arcovito, R. Castagnola, G. Fratocchi, A. Mordente, *et al.*, Oral Mucosa Models to Evaluate Drug Permeability, *Pharmaceutics*, 2023, **15**(5), 1559.

10 A. G. De Boer, L. G. De Leede and D. D. Breimer, Drug absorption by sublingual and rectal routes, *Br. J. Anaesth.*, 1984, **56**(1), 69–82.

11 M. Gibaldi and J. L. Kanig, Absorption of Drugs Through the Oral Mucosa, *J. Oral Ther. Pharmacol.*, 1965, **1**, 440–450.

12 H. Jones and K. Rowland-Yeo, Basic Concepts in Physiologically Based Pharmacokinetic Modeling in Drug Discovery and Development, *CPT: Pharmacometrics Syst. Pharmacol.*, 2013, **2**(8), e63.

13 E. Boger and O. Wigström, A Partial Differential Equation Approach to Inhalation Physiologically Based Pharmacokinetic Modeling, *CPT: Pharmacometrics Syst. Pharmacol.*, 2018, **7**(10), 638–646.

14 M. K. Ladumor and J. D. Unadkat, Predicting Regional Respiratory Tissue and Systemic Concentrations of Orally Inhaled Drugs through a Novel PBPK Model, *Drug Metab. Dispos.*, 2022, **50**(5), 519–528.

15 E. Boger, N. Evans, M. Chappell, A. Lundqvist, P. Ewing, A. Wigenborg, *et al.*, Systems Pharmacology Approach for Prediction of Pulmonary and Systemic Pharmacokinetics and Receptor Occupancy of Inhaled Drugs, *CPT: Pharmacometrics Syst. Pharmacol.*, 2016, **5**(4), 201–210.

16 N. Hartung and J. M. Borghardt, A mechanistic framework for a priori pharmacokinetic predictions of orally inhaled drugs, *PLoS Comput. Biol.*, 2020, **16**(12), e1008466.

17 T. Yaksh and M. Wallace, Opioids, Analgesia, and Pain Management, in *Goodman & Gilman's: The Pharmacological Basis of Therapeutics [Internet]*, ed. L. L. Brunton, R. Hilal-Dandan and B. C. Knollmann, McGraw-Hill Education, New York, NY, 13th edn, 2017, [cited 2025 Sept 18]. Available from: accessanesthesiology.mhmedical.com/content.aspx?aid=1162536611.

18 L. Pande and B. Piper, An Examination of the Complex Pharmacological Properties of the Non-Selective Opioid Receptor Modulator Buprenorphine [Internet], Preprints, 2020, [cited 2025 Aug 14]. Available from: https://www.preprints.org/manuscript/202011.0443/v1.

19 R. P. Nath, R. A. Upton, E. T. Everhart, P. Cheung, P. Shwonek, R. T. Jones, *et al.*, Buprenorphine pharmacokinetics: relative bioavailability of sublingual tablet and liquid formulations, *J. Clin. Pharmacol.*, 1999, **39**(6), 619–623.

20 R. Dong, H. Wang, D. Li, L. Lang, F. Gray, Y. Liu, *et al.*, Pharmacokinetics of Sublingual Buprenorphine Tablets Following Single and Multiple Doses in Chinese Participants With and Without Opioid Use Disorder, *Drugs R & D*, 2019, **19**(3), 255–265.

21 J. Mendelson, R. A. Upton, E. T. Everhart, P. J. Iii and R. T. Jones, Bioavailability of Sublingual Buprenorphine, *J. Clin. Pharmacol.*, 1997, **37**(1), 31–37.

22 D. S. Harris, J. E. Mendelson, E. T. Lin, R. A. Upton and R. T. Jones, Pharmacokinetics and Subjective Effects of Sublingual Buprenorphine, Alone or in Combination with Naloxone, *Clin. Pharmacokinet.*, 2004, **43**(5), 329–340.

23 H. McQuay and R. Moore, *Buprenorphine kinetics in humans. Buprenorphine: Combating Drug Abuse with a Unique Opioid New York*, Wiley-Liss, 1995, pp. 137–147.

24 A. Elkader and B. Sproule, Buprenorphine, *Clin. Pharmacokinet.*, 2005, **44**(7), 661–680.

25 J. J. Jr Kuhlman, S. Lalani, J. Jr Magluilo, B. Levine, W. D. Darwin, R. E. Johnson, *et al.*, Human Pharmacokinetics of Intravenous, Sublingual, and Buccal Buprenorphine*, *J. Anal. Toxicol.*, 1996, **20**(6), 369–378.

26 P. Marquet, Pharmacology of High-Dose Buprenorphine, in *Buprenorphine Therapy of Opiate Addiction [Internet]*, ed. P. Kintz and P. Marquet, Humana Press, Totowa, NJ, 2002, p. 1–11, [cited 2025 Aug 15]. DOI: 10.1007/978-1-59259-282-1_1.

27 M. v. Hoogdalem, R. Tanaka, T. N. Johnson, A. A. Vinks and T. Mizuno, Development and Verification of a Full Physiologically Based Pharmacokinetic Model for Sublingual Buprenorphine in Healthy Adult Volunteers that Accounts for Nonlinear Bioavailability, *Drug Metab. Dispos.*, 2024, **52**(8), 785–796.

28 H. V. Kalluri, H. Zhang, S. N. Caritis and R. Venkataramanan, A physiologically based pharmacokinetic modelling approach to predict buprenorphine pharmacokinetics following intravenous and sublingual administration, *Br. J. Clin. Pharmacol.*, 2017, **83**(11), 2458–2473.

29 T. B. Nnanna, Clinical Therapy Dose Optimization of Sublingual Buprenorphine in Poorly Adherent Pregnant Patients: A PBPK Translational Modelling Study, *Int. J. Pharm. Chem.*, 2024, **10**(4), 46–79.

30 M. W. van Hoogdalem, T. N. Johnson, B. T. McPhail, S. Kamatkar, S. L. Wexelblatt, L. P. Ward, *et al.*, Physiologically-Based Pharmacokinetic Modeling to Investigate the Effect of Maturation on Buprenorphine Pharmacokinetics in Newborns with Neonatal Opioid Withdrawal Syndrome, *Clin. Pharmacol. Ther.*, 2022, **111**(2), 496–508.

31 H. Zhang, H. V. Kalluri, J. R. Bastian, H. Chen, A. Alshabi, S. N. Caritis, *et al.*, Gestational changes in buprenorphine exposure: A physiologically-based pharmacokinetic analysis, *Br. J. Clin. Pharmacol.*, 2018, **84**(9), 2075–2087.

32 A. Bouchikhi, M. H. Becquemin, J. Bignon, M. Roy and A. Teillac, Particle size study of nine metered dose inhalers,

and their deposition probabilities in the airways, *Eur. Respir. J.*, 1988, **1**(6), 547–552.

33 C. Darquenne, Deposition Mechanisms, *J. Aerosol Med. Pulm. Drug Delivery*, 2020, **33**(4), 181–185.

34 S. Willmann, K. Thelen, C. Becker, J. B. Dressman and J. Lippert, Mechanism-based prediction of particle size-dependent dissolution and absorption: Cilostazol pharmacokinetics in dogs, *Eur. J. Pharm. Biopharm.*, 2010, **76**(1), 83–94.

35 N. M. Hagelberg, M. Fihlman, T. Hemmilä, J. T. Backman, J. Laitila, P. J. Neuvonen, *et al.*, Rifampicin decreases exposure to sublingual buprenorphine in healthy subjects, *Pharmacol. Res. Perspect.*, 2016, **4**(6), e00271.

36 J. G. Wojtyniak, H. Britz, D. Selzer, M. Schwab and T. Lehr, Data Digitizing: Accurate and Precise Data Extraction for Quantitative Systems Pharmacology and Physiologically-Based Pharmacokinetic Modeling, *CPT: Pharmacometrics Syst. Pharmacol.*, 2020, **9**(6), 322–331.

37 Y. Zhang, M. Huo, J. Zhou and S. Xie, PKSolver: An add-in program for pharmacokinetic and pharmacodynamic data analysis in Microsoft Excel, *Comput. Methods Programs Biomed.*, 2010, **99**(3), 306–314.

38 E. Weibel and D. M. Gomez, Architecture of the human lung, *Science*, 1962, **137**, 577–585.

39 M. Pellowe, *Inhalation-model/configure_inhalation_parameters.R at main · Open-Systems-Pharmacology/Inhalation-model [Internet]*, St Clements Canada: Open Systems Pharmacology, 2023, [cited 2025 Aug 21]. Available from: https://github.com/Open-Systems-Pharmacology/Inhalation-model/blob/main/configure_inhalation_parameters.R.

40 J. Mazurek, M. Hoffmann, A. Fernandez Casares, P. D. Cox and M. D. Minardi, Buprenorphine [Internet]. 2014 [cited 2025 Sept 18]. Available from: https://www.crystallography.net/cod/2239524.html.

41 PubChem. Buprenorphine [Internet]. [cited 2025 Sept 18]. Available from: https://pubchem.ncbi.nlm.nih.gov/compound/644073.

42 Buprenorphine [Internet]. [cited 2025 Sept 19]. Available from: https://go.drugbank.com/drugs/DB00921.

43 A. Avdeef, D. A. Barrett, P. N. Shaw, R. D. Knaggs and S. S. Davis, Octanol−, Chloroform−, and Propylene Glycol Dipelargonat−Water Partitioning of Morphine-6-glucuronide and Other Related Opiates, *J. Med. Chem.*, 1996, **39**(22), 4377–4381.

44 R. E. S. Bullingham, H. J. McQuay, A. Moore and M. R. D. Bennett, Buprenorphine kinetics, *Clin. Pharmacol. Ther.*, 1980, **28**(5), 667–672.

45 Y. Takahashi, N. Ishii, H. Arizono, S. Nishimura, K. Tsuruta, N. Saito, *et al.*, Pharmacokinetics of Buprenorphine Hydrochloride (BN HCl) (1): Absorption, distribution, metabolism and excretion of BN HCl in rats when administered subcutaneously or transdermally (TSN-09: tape containing BN HCl), *Xenobiot. Metab. Dispos.*, 2001, **16**(6), 569–583.

46 K. Thelen, K. Coboeken, S. Willmann, R. Burghaus, J. B. Dressman and J. Lippert, Evolution of a detailed physiological model to simulate the gastrointestinal transit and absorption process in humans, Part 1: Oral solutions, *J. Pharm. Sci.*, 2011, **100**(12), 5324–5345.

47 H. Wen, M. W. Sadiq, L. E. Friberg and E. M. Svensson, Translational Physiologically Based Pharmacokinetic Modeling to Predict Human Pulmonary Kinetics After Lung Delivery, *CPT: Pharmacometrics Syst. Pharmacol.*, 2025, **14**(4), 796–806.

48 A. Rescigno, J. S. Beck and A. K. Thakur, The use and abuse of models, *J. Pharmacokinet. Biopharm.*, 1987, **15**(3), 327–340.

49 D. A. Ciraulo, R. J. Hitzemann, E. Somoza, C. M. Knapp, J. Rotrosen, O. Sarid-Segal, *et al.*, Pharmacokinetics and Pharmacodynamics of Multiple Sublingual Buprenorphine Tablets in Dose-Escalation Trials, *J. Clin. Pharmacol.*, 2006, **46**(2), 179–192.

50 M. C. Chawarski, D. E. Moody, J. Pakes, P. G. O'Connor and R. S. Schottenfeld, Buprenorphine tablet versus liquid: a clinical trial comparing plasma levels, efficacy, and symptoms, *J. Subst. Abuse Treat.*, 2005, **29**(4), 307–312.

51 J. Mendelson, R. A. Upton, E. T. Everhart, P. J. Iii and R. T. Jones, Bioavailability of Sublingual Buprenorphine, *J. Clin. Pharmacol.*, 1997, **37**(1), 31–37.

52 S. D. McAleer, R. J. Mills, T. Polack, T. Hussain, P. E. Rolan, A. D. Gibbs, *et al.*, Pharmacokinetics of high-dose buprenorphine following single administration of sublingual tablet formulations in opioid naïve healthy male volunteers under a naltrexone block, *Drug Alcohol Depend.*, 2003, **72**(1), 75–83.

53 D. E. Moody, W. B. Fang, J. Morrison and E. McCance-Katz, Gender differences in pharmacokinetics of maintenance dosed buprenorphine, *Drug Alcohol Depend.*, 2011, **118**(2–3), 479–483.

54 U.S. Food and Drug Administration, Draft Guidance for Industry: Drug Interaction Studies—Study Design, Data Analysis, Implications for Dosing, and Labeling Recommendations. U.S. Department of Health and Human Services Food and Drug Administration Center for Drug Evaluation and Research (CDER). 2012. Available at: https://downloads.regulations.gov/FDA-2006-D-0036-0032/content.pdf (Accessed: 09 August 2025).

55 M. W. van Hoogdalem, R. Tanaka, T. N. Johnson, A. A. Vinks and T. Mizuno, Development and Verification of a Full Physiologically Based Pharmacokinetic Model for Sublingual Buprenorphine in Healthy Adult Volunteers that Accounts for Nonlinear Bioavailability, *Drug Metab. Dispos.*, 2024, **52**(8), 785–796.

56 N. R. Labiris and M. B. Dolovich, Pulmonary drug delivery. Part I: Physiological factors affecting therapeutic effectiveness of aerosolized medications, *Br. J. Clin. Pharmacol.*, 2003, **56**(6), 588–599.

57 H. Majid, W. Hofmann and R. Winkler-Heil, Comparison of Stochastic Lung Deposition Fractions with Experimental Data, *Ann. Occup. Hyg.*, 2012, **56**(3), 278–291.

58 D. Arora, J. Peart and P. R. Byron, USA market 1990–2005 : products and instructions for use, in *Respiratory Drug Delivery 2006*, ed. R. N. Dalby, P. R. Byron, J. Peart,

J. D. Suman and S. J. Farr, Davis Healthcare International, IL, USA, 2006, pp. 955–959.

59 OECD. Guidance Document on the Characterisation, Validation and Reporting of Physiologically Based Kinetic (pbk) Models for Regulatory Purposes. OECD Series on Testing and Assessment, No. 331, OECD Series on Testing and Assessment 103. (2021).

60 H. J. Clewell III, M. B. Reddy, T. Lave and M. E. Andersen, Physiologically Based Pharmacokinetic Modeling, in *Preclinical Development Handbook: ADME and Biopharmaceutical Properties, Pharmaceutical Development Series*, ed. S. C. Gad, 2008, pp. 1165–1225.

61 M. Holz and A. Fahr, Compartment modeling, *Adv. Drug Delivery Rev.*, 2001, **48**(2), 249–264.

62 E. J. Cone, S. L. Dickerson, W. D. Darwin, P. Fudala and R. E. Johnson, Elevated drug saliva levels suggest a 'depot-like' effect in subjects treated with sublingual buprenorphine, *NIDA Res. Monogr.*, 1990, **105**, 569.

63 R. Bullingham, H. McQuay, E. Porter, M. Allen and R. Moore, Sublingual buprenorphine used postoperatively: ten hour plasma drug concentration analysis, *Br. J. Clin. Pharmacol.*, 1982, **13**(5), 665–673.

64 J. N. Moore, M. R. Gastonguay, C. M. Ng, S. C. Adeniyi-Jones, D. E. Moody, W. B. Fang, *et al.*, The Pharmacokinetics and Pharmacodynamics of Buprenorphine in Neonatal Abstinence Syndrome, *Clin. Pharmacol. Ther.*, 2018, **103**(6), 1029–1037.